

Inhibition of a biological sulfide oxidation under haloalkaline conditions by thiols and diorgano polysulfanes

Roman, Pawel; Lipińska, Joanna; Bijmans, Martijn F M; Sorokin, D.; Keesman, Karel J.; Janssen, Albert J H

DOI

[10.1016/j.watres.2016.06.003](https://doi.org/10.1016/j.watres.2016.06.003)

Publication date

2016

Document Version

Accepted author manuscript

Published in

Water Research

Citation (APA)

Roman, P., Lipińska, J., Bijmans, M. F. M., Sorokin, D., Keesman, K. J., & Janssen, A. J. H. (2016). Inhibition of a biological sulfide oxidation under haloalkaline conditions by thiols and diorgano polysulfanes. *Water Research*, 101, 448-456. <https://doi.org/10.1016/j.watres.2016.06.003>

Important note

To cite this publication, please use the final published version (if applicable). Please check the document version above.

Copyright

Other than for strictly personal use, it is not permitted to download, forward or distribute the text or part of it, without the consent of the author(s) and/or copyright holder(s), unless the work is under an open content license such as Creative Commons.

Takedown policy

Please contact us and provide details if you believe this document breaches copyrights. We will remove access to the work immediately and investigate your claim.

1 **Inhibition of a biological sulfide oxidation under haloalkaline**
2 **conditions by thiols and diorgano polysulfanes**
3
4

5 Pawel Roman,^{*,a,b} Joanna Lipińska,^{b,c} Martijn F.M. Bijmans,^b Dimitry Y. Sorokin,^{d,e} Karel J.
6 Keesman,^{b,f} Albert J.H. Janssen^{a,g}
7

8 ^a Sub-department of Environmental Technology, Wageningen University, P.O. Box 17, 6700
9 AA Wageningen, the Netherlands

10 ^b Wetsus, European Centre of Excellence for Sustainable Water Technology, Oostergoweg 9,
11 8911 MA Leeuwarden, the Netherlands

12 ^c Faculty of Chemistry, Warsaw University of Technology, Noakowskiego St. 3, 00-664
13 Warsaw, Poland

14 ^d Winogradsky Institute of Microbiology, Research Centre of Biotechnology, Russian
15 Academy of Sciences, Prospect 60-let Oktyabrya 7/2, 117811 Moscow, Russia

16 ^e Department of Biotechnology, Delft University of Technology, Julianalaan 67, 2628 BC
17 Delft, The Netherlands

18 ^f Biobased Chemistry & Technology, Wageningen University, P.O. Box 17, 6700 AA
19 Wageningen, The Netherlands

20 ^g Shell Technology Centre Bangalore, RMZ Centennial Campus B, Kundalahalli Main Road,
21 Bengaluru 560 048 India
22

23 * Corresponding author. Phone: +31 (0)317 483339; fax: +31 (0)317 482108; E-mail address:
Pawel.Roman@wetsus.nl. Sub-department of Environmental Technology, Wageningen
University, P.O. Box 17, 6700 AA Wageningen, the Netherlands

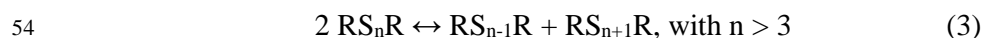
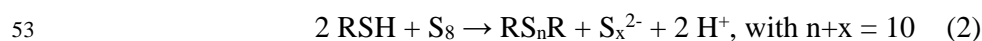
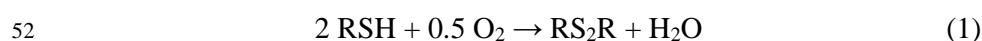
24 **Abstract**

25 A novel approach has been developed for the simultaneous description of sulfur and sulfate
26 formation from the biological oxidation of hydrogen sulfide (H₂S) using a quick, sulfide-
27 dependent respiration test. Next to H₂S, thiols are commonly present in sour gas streams. We
28 investigated the inhibition mode and the corresponding inhibition constants of six thiols and
29 diorgano polysulfanes on the biological oxidation of H₂S. A linear relationship was found
30 between the calculated IC₅₀ values and the lipophilicity of the inhibitors. Moreover,
31 a mathematical model was proposed to estimate the biomass activity in the absence and
32 presence of sulfurous inhibitors. The biomass used in the respiration tests originated from
33 a full-scale biodesulfurization reactor. A microbial community analysis of this biomass
34 revealed that two groups of microorganism are abundant, viz. *Ectothiorhodospiraceae* and
35 *Piscirickettsiaceae*.

36 1. Introduction

37 Biological processes to remove hydrogen sulfide (H₂S) from gas streams have become
38 increasingly attractive in recent years as an alternative to physicochemical technologies
39 (Janssen et al. 2009; Schieder et al. 2003). Key drivers to select biotechnological solutions for
40 the treatment of sour gas streams instead of physicochemical processes are the higher H₂S
41 removal efficiencies, lower operational cost and, most importantly, the simpler operating
42 procedures (Cline et al. 2003). After the first commercial applications in the oil and gas
43 industry, the need has arisen to broaden the operating window of these bioprocesses by
44 enabling the removal of thiols next to H₂S as these volatile organosulfur compounds are
45 regularly present in sour natural gas streams.

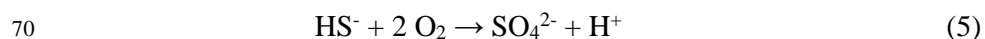
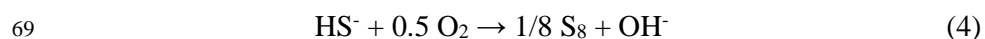
46 Thiols are considerably more toxic to sulfur oxidizing bacteria (SOB) than dissolved
47 sulfide (Roman et al. 2015b; van den Bosch et al. 2009). In the presence of oxygen thiols are
48 rapidly oxidized to organic disulfides (Eq. 1) (van Leerdam et al. 2011). Thiols also react with
49 biologically produced sulfur particles to form diorgano polysulfanes (Eq. 2). These
50 organosulfur compounds (with n > 3) are unstable and quickly decompose to stable di- and
51 trisulfides (Steudel 2002), according to Eq. 3.



55 Diorgano di- and trisulfides are found to be the most predominant organosulfur compounds in
56 a bioreactor operating at haloalkaline conditions (Roman et al. 2015b). Clearly, a better
57 understanding of the toxic effects of these compounds on SOB is of key importance to ensure
58 a stable reactor performance.

59 It was shown that *Thioalkalivibrio sulfidophilus* is the most dominant SOB in
60 full-scale Thiopaq installations that are operated at haloalkaline conditions, i.e. at pH 9, 1 M

61 total Na^+ and at a redox potential below -250 mV to ensure sulfur-producing conditions
62 (Sorokin et al. 2012). Based on a complete genome analysis Muyzer et al. (2011)
63 reconstructed a sulfur oxidation pathway in *Tv. sulfidophilus*. In this pathway SOB oxidize
64 sulfide to sulfate via zero-valent sulfur as an intermediate. In the first step *Tv. sulfidophilus*
65 oxidizes sulfide to a polysulfur-containing compound(s), hereafter referred to as $\{\text{S}_x\}$. $\{\text{S}_x\}$
66 can be secreted from the periplasm as elemental sulfur globules at low redox conditions or
67 oxidized to sulfate via intermediate sulfite at elevated redox values (Fig. 1). The reactions
68 describing the formation of both products can be written in the following simplified form:



71 A more detailed description of the underlying principles of biological sulfide oxidation was
72 presented by Klok et al. (2012).

73 Reaction kinetics of the biological sulfide oxidation processes can be studied by
74 performing biological oxygen monitoring (BOM) tests, which are based on monitoring the
75 decrease of the dissolved oxygen concentration. Recently it was found that for biomass
76 samples in which representatives of the genus *Thioalkalivibrio* were identified as the
77 dominating SOB, the oxygen consumption rate can be described by two different reaction
78 rates (Roman et al. 2015b). The first and fast rate (R1) is related to the partial oxidation of
79 sulfide to $\{\text{S}_x\}$, while the second and much lower rate (R2) is related to the further oxidation
80 of $\{\text{S}_x\}$ to sulfate ions (Fig. 1) (Sorokin et al. 2008).

81 We have also shown that by understanding the inhibition mode for a single thiol, it is
82 possible to model the performance of the biodesulfurization process in lab-scale reactors
83 (Roman et al. 2015b). The aim of the current study is to investigate the inhibitory effects of
84 the most common thiols i.e. MT, ethanethiol (ET), 1-propanothiol (PT) and the products of
85 their chemical oxidation (Eq. 1-3): DMDS, diethyl disulfide (DEDS) and dipropyl disulfide

86 (DPDS) on the biological oxidation rate of dissolved sulfide. The identified modes of
87 inhibition and the associated kinetic parameters will be used in a set of mathematical
88 equations to describe the prevailing reaction kinetics in integrated systems for the treatment of
89 sulfide and thiols containing gas streams. Several authors have presented kinetic models to
90 characterize the aerobic biological sulfide oxidation process (Mora et al. 2016; Klok et al.
91 2013; Roosta et al. 2011). However, the inhibition by organic sulfur compounds was never
92 taken into account despite the fact that thiols are a commonly present in sour gas streams (Cui
93 et al. 2009; Lee et al. 2006; Kim et al. 2005). Our mathematical model builds on a genomic
94 model proposed by Muyzer et al. (2011). The presented model can be used as a tool for
95 designing industrial biodesulfurization installations.

96

97 **2. Materials and methods**

98 ***2.1. Experimental setup***

99 Respiration tests were performed to assess the kinetic parameters of biological sulfide
100 oxidation and the mode of inhibition by thiols and diorgano polysulfanes (Table 1) in an air-
101 saturated medium. We used a similar setup as described elsewhere (Kleinjan et al. 2005),
102 which consisted of a glass mini-reactor (60 mL) equipped with a magnetic stirrer. The reactor
103 was closed with a Teflon piston to avoid any oxygen ingress. We added stock solutions
104 containing the inhibitors and sulfide to the reactor with a syringe passing through the piston.
105 The sulfide oxidation rate was determined by measuring the oxygen consumption rate with a
106 dissolved-oxygen (DO) sensor (Oxymax COS22D, Endress+Hauser). Signals from the DO
107 sensor were recorded using a multiparameter transmitter (Liquiline CM442; Endress+Hauser,
108 the Netherlands). All experiments were performed at 35 °C (DC10-P5/U thermostat bath,
109 Haake, Germany)(Roman et al. 2015a; Graaff 2012; van den Bosch et al. 2009).

110

111 **2.2. Medium composition**

112 The reactor medium included a carbonate/bicarbonate buffer of 0.1 M Na₂CO₃ and 0.8
113 M NaHCO₃ (1 M total Na⁺). Furthermore, the medium contained 1.0 g K₂HPO₄, 0.20 g
114 MgCl₂ × 6 H₂O, and 0.60 g urea, each per 1 L of Milli-Q water. A trace elements solution
115 (1 mL L⁻¹) was added as described elsewhere (Pfennig and Lippert 1966). The final pH of the
116 medium was 9 at 35 °C.

117

118 **2.3. Biomass**

119 In the respiration tests we used biomass sampled from a full-scale gas
120 biodesulfurization installation, located at Industriewater Eerbeek B.V., the Netherlands which
121 is operated at oxygen-limiting conditions and low redox potential values (Janssen et al. 2009).

122 A sulfur-free biomass suspension was prepared by centrifugation (30 min at 16,000 x
123 g) of the sulfide-oxidizing culture followed by a washing step after re-suspending the pellet in
124 the same medium as described in section 2.2.

125 DNA extraction from biomass samples taken from a full-scale gas biodesulfurization
126 installation were performed as follows. First, the samples were washed twice with a buffer of
127 pH 9 and 0.5 M Na⁺ to prevent the occurrence of an osmotic shock. Then, the washing was
128 performed by (1) centrifuging the samples at 20,000 x g for 5 min; (2) removal of the
129 supernatant; and (3) addition of fresh buffer and mixing with a vortex to re-suspend the pellet.
130 Afterwards, Total Genomic DNA was extracted from the washed biomass using the
131 PowerBiofilm™ DNA Isolation Kit (MoBio, USA) following the manufacturer's instructions.
132 All the above procedures were performed in duplicate.

133 For biomass samples from the full-scale gas biodesulfurization installation the 16S
134 rRNA gene profiling was performed as following. Illumina 16S rRNA gene amplicon
135 libraries were generated and sequenced at BaseClear BV (Leiden, the Netherlands). In short,

136 barcoded amplicons from the V3-V4 region of 16S rRNA genes were generated using a 2-step
137 PCR. 10-25 ng genomic DNA was used as template for the first PCR with a total volume of
138 50 μ l using the 341F (5'-CCTACGGGNGGCWGCAG-3') and the 785R (5'-
139 GACTACHVGGGTATCTAATCC-3') primers appended with Illumina adaptor sequences.
140 PCR products were purified and the size of the PCR products were checked on a Bioanalyzer
141 (Agilent, CA, USA) and quantified by fluorometric analysis. Purified PCR products were
142 used for the 2nd PCR in combination with sample-specific barcoded primers. Subsequently,
143 PCR products were purified, checked on a Bioanalyzer (Agilent, CA, USA) and quantified,
144 followed by multiplexing, clustering, and sequencing on an Illumina MiSeq with the paired-
145 end 250 cycles protocol and indexing. The sequencing run was analyzed with Illumina
146 CASAVA pipeline (v1.8.3) with demultiplexing based on sample-specific barcodes. The raw
147 sequencing data produced was processed by removing the sequence reads of too low quality
148 (only "passing filter" reads were selected) and discarding reads containing adaptor sequences
149 or PhiX control with an in-house filtering protocol. A quality assessment on the remaining
150 reads was performed using the FASTQC quality control tool version 0.10.0.

151

152 ***2.4. Respiration tests***

153 Sulfide-dependent O₂-consumption rates were measured in a thermostated reactor
154 (Section 2.1). The biomass concentration was always kept at 10 mg N L⁻¹, measured as the
155 amount of organic nitrogen oxidized to nitrate by digestion with peroxodisulphate (LCK238,
156 Hach Lange, the Netherlands) in triplicate. The medium with biomass was aerated as
157 described elsewhere (van den Bosch et al. 2009). Measurements commenced after sulfide was
158 injected and lasted for 5 to 14 minutes. All solutions containing sulfurous compounds were
159 freshly prepared before each series of experiments. Methanol was used as a solvent for
160 hydrophobic inhibitors (Table 1), which had no effect on the oxygen consumption rate (data

161 not shown). For all other inhibitors, we used Milli-Q water as a solvent. In order to prevent
162 any oxidation of thiols all solvents were first purged with 99.99% nitrogen gas for at least 15
163 min.

164 A wide range of sulfide concentrations was applied to estimate the kinetic parameters
165 for both biological sulfide oxidation rates (R1 and R2, Fig.1). Sulfide concentrations ranging
166 between 0.02 and 0.3 mM were used to estimate kinetic parameters related to R1. In this
167 concentration range R2 was more or less constant and ranges around its maximum value.
168 Hence, a reliable estimation of its value was not possible. In order to estimate kinetic
169 parameters related to R2 significantly lower sulfide concentrations (0.005 - 0.012 mM) were
170 applied. For these ranges of sulfide concentrations, we experimentally verified that the
171 contribution of chemical sulfide oxidation to biological sulfide oxidation is insignificantly
172 small, and can therefore be neglected.

173 We performed a series of experiments in the absence of any inhibitor to estimate the
174 maximum biological sulfide oxidation (r_{max}) rate and the associated Michaelis constant (K_M).
175 The sulfide concentration for R1 varied from 0.2 to 4.0 K_M and for R2 from 2.0 to 8.0 K_M to
176 obtain reliable estimates of K_M and r_{max} (Marangoni 2003). The methylene blue method
177 (Cuvette test LCK653, Hach Lange, the Netherlands) was used to verify the sulfide
178 concentration in stock solution. All measurements were performed in triplicate. We
179 performed respiration tests in the presence of an inhibitor to identify the mode of inhibition
180 and the parameters for inhibitors that bind to free enzyme (K_i) and enzyme-substrate complex
181 (K_{ies}). In these tests first the inhibitor was added and then the substrate. Each series of
182 experiments was carried out in duplicate. We tested all inhibitors for both oxidation steps (R1
183 and R2) at 35 °C with an incubation time between 1 and 60 min to determine the time
184 required for biomass incubation with an inhibitor at a certain concentration.

185

2.5. Modelling biological sulfide oxidation pathway

A mathematical model for describing the biological sulfide oxidation with SOB has been developed on the basis of material balances for sulfide, $\{S_x\}$ and O_2 . It has been assumed that in the absence of inhibitors SOB oxidize sulfide (Eq. 6-7) to $\{S_x\}$ (Eq. 8). The formed $\{S_x\}$ is transformed to sulfate which results in an additional oxygen consumption (Eq. 9).

$$\frac{dc_{HS}}{dt} = -c_b \gamma^{R1} \frac{r_{max}^{R1} c_{HS}}{K_M^{R1} + c_{HS}} \quad (6)$$

$$\frac{dc_{O_2}^{R1}}{dt} = -c_b \frac{r_{max}^{R1} c_{HS}}{K_M^{R1} + c_{HS}} \quad (7)$$

$$\frac{dc_{S_x}}{dt} = c_b \gamma^{R1} \frac{r_{max}^{R1} c_{HS}}{K_M^{R1} + c_{HS}} - c_b \gamma^{R2} \frac{r_{max}^{R2} c_{S_x}}{K_M^{R2} + c_{S_x}} \quad (8)$$

$$\frac{dc_{O_2}^{R2}}{dt} = -c_b \frac{r_{max}^{R2} c_{S_x}}{K_M^{R2} + c_{S_x}} \quad (9)$$

The superscripts $R1$ and $R2$ refer to the first and second oxidation rate, as shown in Figure 1.

The model also includes the endogenous oxygen consumption (r_{eg}) (van den Bosch et al. 2009), which was calculated as follows:

$$\frac{dc_{O_2}^{eg}}{dt} = -r_{eg} \quad (10)$$

Biomass growth is not included in the model equations as we assume that it remains constant during the relatively short time frame (<14 min) of the respiration experiments (Roman et al. 2015a). It should be noted that the terms used for describing the sulfide and $\{S_x\}$ consumption rates have the same unit, because sulfide is transformed to $\{S_x\}$. The yield coefficients for sulfide (γ^{R1} , mM HS^- (mM O_2)⁻¹) and $\{S_x\}$ consumption (γ^{R2} , mM HS^- (mM O_2)⁻¹) account for the conversion of r_{max} for oxygen consumption to sulfide consumption. It is not possible to estimate $\gamma^{R1,R2}$ and $r_{max}^{R1,R2}$ independently, as they always appear as the algebraic product $\gamma \cdot r_{max}$. Therefore, the values for $\gamma^{R1,R2}$ were chosen from the stoichiometric equations 4 and 5 and in, what follows, only $r_{max}^{R1,R2}$ and the affinity constants in Eq. 6-9 were estimated from the experimental data. Furthermore, it is assumed that oxygen is not a limiting factor as the

209 medium is air-saturated i.e. there is an excess amount of oxygen available and the affinity
 210 constant for oxygen-respiring SOB are in the range of a few μM (Zannoni and others 2004).
 211 BOM tests with sulfide as substrate showed values of 1.5-2.5 $\mu\text{M O}_2$ for the representatives of
 212 the genus *Thioalkalivibrio* (unpublished results). The general mass balances for the substrates
 213 and $\{S_x\}$ are solved for the following range of initial experimental conditions:

$$214 \quad c_{HS}(0) \in [0.003, 0.3] \quad (11)$$

$$215 \quad c_{Sx}(0) = 0 \quad (12)$$

$$216 \quad c_{O_2}^{R1}(0) \in [0.01, 0.022] \quad (13)$$

$$217 \quad c_{O_2}^{R2}(0) = 0 \quad (14)$$

218 Furthermore, c_{HS} , c_{Sx} and c_{O_2} are the concentrations (in mM) of sulfide, $\{S_x\}$ and oxygen,
 219 respectively. The total oxygen consumption is given by:

$$220 \quad c_{O_2}^{tot} = c_{O_2}^{R1} + c_{O_2}^{R2} + c_{O_2}^{eg} \quad (15)$$

221 An uncertainty assessment of the predicted model output was performed by using a
 222 Monte Carlo simulation technique with parameters sampled from the distribution space of the
 223 estimated parameters. For each estimated parameter 100 samples were drawn, leading to 100
 224 sampled parameter vectors. For each vector, we calculated the corresponding model output
 225 trajectory. Based upon the 100 model output trajectories, the mean and the time-varying
 226 standard deviation of the model output were calculated.

227

228 **2.6. Estimation of kinetic parameters**

229 We estimated the kinetic parameters in Eq. 6-9 by using a static approach in which a
 230 stepwise method was taken to minimize the residual error (Marangoni 2003). Firstly, we
 231 estimated r_{max} and K_M from experimental data in the absence of an inhibitor for both R1 and
 232 R2. Secondly, the estimated parameters (r_{max} and K_M) were substituted into a modified

233 “Michaelis-Menten” equation that describes the mode of inhibition, to estimate the inhibition
234 constants (K_i and K_{ies}).

235 To estimate the kinetic parameters related to R2, we had to assume the initial sulfide
236 concentrations instead of $\{S_x\}$ concentrations as it is not possible to measure the
237 intracellularly bonded $\{S_x\}$. To evaluate the effect of this choice we additionally estimated
238 parameters (r_{max} , K_M , and when applicable the inhibition constants: K_i and K_{ies}) using a
239 dynamic approach which relies on solving the relevant set of differential equations (Eq. 6-10)
240 iteratively. In this approach the $\{S_x\}$ concentration is implicitly calculated from the proposed
241 and validated model (Section 3.4). In particular, we solved the following optimization
242 problem:

$$243 \quad \min \sum (c_{O_2}^{tot}(t) - \widehat{c_{O_2}^{tot}}(t, \theta))^2 \quad (16)$$

244 with $\widehat{c_{O_2}^{tot}}$ the calculated total oxygen concentration (Eq. 15), given the solutions to Eq. 6-10
245 for the set of kinetic parameters (θ : r_{max} , K_M). In the presence of inhibitors (Eq. 17-19) the set
246 of parameters is extended with the inhibition constants: K_i and K_{ies} . Given the observations of
247 $c_{O_2}^{tot}$, the kinetic parameters were estimated using a non-linear least-squares method
248 (Levenberg-Marquardt algorithm), as described by Keesman (2011).

249

250

251 **3. Results and discussion**

252 ***3.1. Microbial diversity in a full-scale gas biodesulfurization installation***

253 Microbial community analysis of biomass collected from a full-scale gas
254 biodesulfurization installation in Eerbeek (the Netherlands) showed that the bacterial
255 composition (Supplementary Information, Fig. S1) is similar to what has been described
256 previously (Sorokin et al. 2012). The dominant bacterial group (approximately 50% of the
257 16S rRNA sequences analyzed) belongs to the family *Ectothiorhodospiraceae*. Within this

258 group, 99% of the 16S rRNA sequences belonged to the genus *Thioalkalivibrio*. Also bacteria
259 related to the family *Piscirickettsiaceae* are abundant, 24.8% and 26.1% in both replicates.
260 Within this group, approximately 80% of the 16S rRNA sequences are closely related to the
261 *Thiomicrospira pelophila*/*Thioalkalimicrobium* cluster, which are often present in the full-
262 scale Thiopaq installations (Sorokin et al. 2011).

263

264 **3.2. Determination of incubation time**

265 A complete saturation of enzymes with an inhibitor is required in order to properly
266 determine the inhibition constants (K_i and K_{ies}). Zhang et al. (2001) indicated that in the
267 presence of an inhibitor the incubation time needed to reach complete saturation is related to
268 the inhibitor concentration which, in turn, is related to the degree of inhibition. Due to
269 different susceptibilities of R1 and R2 to the inhibitors (Roman et al. 2015a) it was necessary
270 to apply different inhibitor concentrations, i.e. a higher and a lower one for respectively R1
271 and R2 (Fig.1). The concentration of each inhibitor was chosen such that only partial
272 inhibition was achieved. An appropriate incubation time for each concentration of each
273 inhibitor had to be determined whilst taking into account that too long incubation times for
274 thiols shall be avoided in order to prevent any chemical oxidation to disulfides (Eq. 1).

275 From the results shown in Figure 2 it follows that R1 and R2 require different
276 incubation times to reach a complete saturation of the enzymes in the presence of an inhibitor.
277 Table 2 shows the inhibitor concentrations and incubation times that were selected in the
278 remainder of this study.

279

280 **3.3. Determination of inhibition mode and kinetic parameters**

281 The results from sulfide-dependent respiration tests were plotted in double-reciprocal
282 plots (Supplementary Information, Fig. S2) to identify the inhibition mode related to R1 and

283 R2. From this plot it clearly follows that MT, ET and PT act as competitive inhibitors for R1.
 284 Therefore, the mode of inhibition can be described by a modified “Michaelis-Menten”
 285 equation:

$$286 \quad r_i^{R1} = \frac{r_{max}^{R1} c_{HS}}{K_M^{R1} \left(1 + \frac{c_i}{K_i^{R1}}\right) + c_{HS}} \quad (17)$$

287 where c_i is an inhibitor concentration. This mode of inhibition is in agreement with our
 288 previous findings viz. that MT acts as a competitive inhibitor for sulfide oxidation by SOB
 289 (Roman et al. 2015a). According to Wilms et al. (1980), this can be explained by the
 290 structural similarity between sulfide (HS^-) and MT (CH_3S^-). In contrast, diorgano disulfides
 291 are non-competitive inhibitors for R1 and their inhibitory effects can be described as follows:

$$292 \quad r_i^{R1} = \frac{r_{max}^{R1} c_{HS}}{K_M^{R1} + c_{HS} \left(1 + \frac{c_i}{K_{ies}^{R1}}\right)} \quad (18)$$

293 This type of inhibition is common in multi-substrate reactions (Eq. 4-5) in contrast to single-
 294 substrate reactions (Segal 1993).

295 To establish the effect of thiols and diorgano polysulfanes on R2, double reciprocal
 296 plots were prepared which show a mixed type of inhibition (Supplementary Information, Fig.
 297 S2), indicating that the inhibitors are able to bind at the active and allosteric site of enzymes.
 298 The corresponding specific reaction rate is given by:

$$299 \quad r_i^{R2} = \frac{r_{max}^{R2} c_{HS}}{K_M^{R2} \left(1 + \frac{c_i}{K_i^{R2}}\right) + c_{HS} \left(1 + \frac{c_i}{K_{ies}^{R2}}\right)} \quad (19)$$

300 It is obvious that equations 17-19 only describe a phenomenological characterization of the
 301 experimental observation but do not provide any underlying mechanisms. However, in section
 302 3.4, we will describe that the lipophilicity effects of the inhibitors influence the inhibition of
 303 sulfide oxidation. Then, the specific reaction rates (Eq. 17-19) can substitute the generic rates
 304 mentioned (Eq. 6-9) to predict the biomass activity in the presence of thiols and diorgano
 305 polysulfanes.

306 After unrevealing the mode of inhibition for each inhibitor on R1 and R2, it was
307 possible to estimate the kinetic parameters in equations 17-19. Estimated values of r_{max} , K_M ,
308 K_i and K_{ies} and the corresponding standard deviations are shown in Table 3. From these
309 parameter estimations it follows that MT is the most toxic thiol as it has the lowest K_i value.
310 This is in agreement with our hypothesis that the inhibitory effect decreases with increasing
311 steric hindrance of the thiols (Roman et al. 2015a). Estimated values of K_{ies} for R1 and
312 diorgano polysulfanes are strongly correlated with their molecular weight ($R^2 = 0.999$).
313 Similar strong correlations are observed for K_i and K_{ies} of thiols and for K_i of diorgano
314 polysulfanes for R2. However, K_{ies} of diorgano polysulfanes is more or less constant
315 (approximately 0.24 mM), indicating that the same non-competitive inhibition mechanism
316 applies. Because the diorgano polysulfanes in our tests only differ in their aliphatic chain
317 length while the number of sulfur atoms remains the same, it can be hypothesized that non-
318 competitive inhibition (K_{ies}) is related to the sulfur-sulfur bond.

319 The results from the parameter estimations show that there is no significant difference
320 between the estimated values obtained via the dynamic and the static approach (data not
321 shown). However, the dynamic approach yields K_m values with a higher level of uncertainty
322 in the estimate because the data contained less information.

323

324

325 **3.4. Calculation of IC_{50} and its correlation with lipophilicity**

326 The IC_{50} value represents the inhibitor concentration at which 50% inhibition occurs
327 of an enzymatic reaction at a specific substrate concentration. A mathematical relation
328 between the inhibition constants and the IC_{50} value is described by Yung-Chi and Prusoff
329 (1973). Equations describing this relationship for competitive, uncompetitive and mixed
330 inhibition are given by:

331
$$IC_{50} = K_i \left(1 + \frac{c_{HS}}{K_M} \right) \quad (20)$$

332
$$IC_{50} = K_{ies} \left(1 + \frac{K_M}{c_{HS}} \right) \quad (21)$$

333
$$IC_{50} = \frac{c_{HS} + K_M}{\frac{K_M}{K_i} + \frac{c_{HS}}{K_{ies}}} \quad (22)$$

334 Based on the estimated values for the kinetic parameters and the corresponding
 335 uncertainties (Table 3), we calculated IC_{50} values with uncertainty bounds for both oxygen
 336 consumption rates (R1 and R2) and for each of the inhibitors (Fig. 3 A-C). Taking into
 337 account that the IC_{50} value is dependent on the substrate concentration, results are plotted in
 338 the range of 0-3 mM sulfide. To compare our results with available literature data, the IC_{50}
 339 values for MT and DMDS for R1 have been reviewed (Table 4). The values for both
 340 inhibitors are very similar to previously reported data. It can be seen that thiols become less
 341 toxic with increasing substrate concentrations (Fig. 3A), while the IC_{50} values for diorgano
 342 polysulfanes stabilize at around 1 mM for substrate concentrations above 0.5 mM (Fig. 3B).
 343 Moreover, it can be observed that R2 is more susceptible to the inhibitors at almost all sulfide
 344 concentrations (Fig. 3C) because of much lower IC_{50} values. These results support our
 345 previous findings from lab-scale reactor experiments that biological production of sulfate is
 346 more vulnerable to inhibitors than the biological production of sulfur (Roman et al. 2015a;
 347 Roman et al. 2015b).

348 It is known that the biological activity of inhibitors can be directly related to their
 349 physicochemical properties (Cronin 2004). Hence, we compared their lipophilicity expressed
 350 as logarithm of octanol-water partition coefficient ($\log(P)$), with the measured IC_{50} values.
 351 The estimation of $\log(P)$ for the various inhibitors was calculated using ALOGPS 2.1
 352 software (Anon n.d.; Tetko and Tanchuk 2002). For thiols the $\log(P)$ values ranged from 0.4
 353 to 1.2 and for diorgano polysulfanes ranged from 1 to 3. To determine whether lipophilicity is
 354 correlated with IC_{50} values at sulfide concentration of 0.2 mM, the relationship between

355 log(P) and IC₅₀ values for the particular group of inhibitors for both oxidation rates (R1 and
356 R2) was assessed by linear regression (Fig. 4 A-B). A clear and positive correlation was
357 found between log(P) and the IC₅₀ values for thiols for both R1 and R2, with coefficients of
358 determination of 0.848 and 0.999, respectively (Fig. 4A). These correlations show that
359 hydrophobic thiols are less toxic to SOB compared to the more hydrophilic ones. This might
360 also indicate that inhibition by thiols is related to the hydrophilic interaction in the inhibition
361 mechanisms. For diorgano polysulfanes, we found large negative correlations between log(P)
362 and the IC₅₀ values with coefficients of determination of 0.995 and 0.994 for R1 and R2,
363 respectively (Fig. 4B). In contrast to thiols, toxicity of diorgano polysulfanes increases with
364 their lipophilicity which suggests involvement of hydrophobic interaction in the inhibition
365 mechanisms. This could mean that diorgano polysulfanes are affecting enzymes that are
366 embedded in the cell membrane which is in agreement with another observation that diorgano
367 polysulfanes toxicity is not competitive for R1 because the substrate, i.e. sulfide, reacts with
368 enzymes located outside the cell membrane in the periplasm or on the external surface of the
369 cell membrane (Gregersen et al. 2011).

370

371 ***3.5. Comparison of the model results with experimental data***

372 The estimated kinetic parameters in Table 3 were obtained from sulfide-dependent
373 respiration tests and then used in the above described mathematical model (Eq. 6-15). The
374 model predictions were compared with a set of independent respirometric results. The
375 biomass used for the validation experiments was taken from the same full-scale reactor but
376 two months after biomass sampling for the parameter estimation tests. The model was
377 experimentally validated in the absence of an inhibitor with the initial sulfide concentration
378 ranging from 0.005 to 0.2 mM (Fig. 5A-F). From these results, it can be seen that the
379 proposed model predicts the oxygen consumption reasonably well for haloalkaliphilic SOB

380 cultivated under O₂-limiting conditions. For the highest sulfide concentrations the deviation
381 between experimental measurements and model predictions increases somewhat which can be
382 attributed to a lag phase of the SOB. Nevertheless, an error analysis of r^{R1} showed that the
383 coefficient of variation was always below $\pm 25\%$, which is a reasonable margin if one takes
384 into account the measurement errors in the dissolved oxygen, sulfide, biomass concentrations,
385 liquid volumes and influence of the error propagation. Furthermore, the measured and
386 predicted reaction rates seem to correspond (Supplementary Information, Fig. S3). The
387 uncertainty in the model output resulting from uncertainties in the estimates for the kinetic
388 parameters (Table 3) is rather small because of strong correlations between the identifiable
389 parameter estimates, as also follows from the covariance and correlation matrix of the
390 estimates (Supplementary Information, S2). In addition, respiration tests with biomass
391 concentration of 1 mg N L⁻¹ were performed to validate the model. Although these tests were
392 performed with ten times lower biomass concentration than tests used for the parameter
393 estimation, no significant differences between the model output and the measured oxygen
394 consumption rate were observed, i.e. the coefficient of variation was below $\pm 27\%$.

395 Hereafter, the model was validated with tests performed at constant initial sulfide
396 concentration (0.03 mM) in the presence of MT, ET and DMDS at different concentrations
397 (Fig. 6A-F). For this purpose, equations describing the model (Eq. 6-15) were adjusted with
398 modified “Michaelis-Menten” equations (Eq. 17-19) depending on the type of inhibitor. For
399 all measurements, model predictions are in a good agreement with the experimental results
400 (on average the difference is $14 \pm 4\%$ for R1 and $7 \pm 6\%$ for R2). This allows for an explicit
401 mathematical description and supports double sulfide-dependent oxygen consumption rates
402 by SOB. Consequently, the model can be used to predict the biomass activity and to predict
403 the accumulation rate of intracellularly produced $\{S_x\}$.

404 From Figure 6 it can be seen that for biological oxidation of sulfide inhibited by MT
405 and ET, the experimental results and the model predictions show almost two times lower
406 sulfide consumption rates and significantly lower oxidation rates of $\{S_x\}$ compared to
407 uninhibited reactions. For reactions inhibited by DMDS, the oxidation of sulfide is inhibited
408 only slightly (8%, Fig. 6E) and moderately (23%, Fig. 6F), while the oxidation of $\{S_x\}$ is
409 almost completely blocked (Fig. 6E-F). These results clearly show that the sulfide oxidation is
410 significantly less vulnerable to these sulfurous inhibitors than $\{S_x\}$ oxidation is. In the
411 presence of an inhibitor model output uncertainties increased due to the uncertainty of
412 inhibition constants (Figure 5).

413

414 **4. Conclusions**

415 In this study, a novel approach for the simultaneous description of biological sulfur
416 and sulfate formation using a quick sulfide-dependent respiration test has been presented. By
417 applying approach, the inhibition of haloalkaliphilic SOB by the most common thiols and
418 their corresponding diorgano polysulfanes was described. We found that IC_{50} values are
419 correlated with the lipophilicity of the inhibitors. Thiols interfere with the oxidation of sulfide
420 by hydrophilic interaction while hydrophobic interaction is the most important mechanism for
421 diorgano polysulfanes. This can be related to the ionic and non-ionic form of the various
422 inhibitors. For each inhibitor, we identified the inhibition mode and the corresponding
423 inhibition constants. Understanding the inhibitory properties of thiols on the biological
424 oxidation of sulfide allows designing full-scale systems in which any inhibition is prevented
425 e.g. by increasing the biomass or/and substrate concentration.

426 Moreover, a mathematical model has been described to calculate the biological sulfide
427 oxidizing capacity in the absence or presence of inhibitory thiols and their corresponding
428 diorgano polysulfanes. The proposed model can be used to design full-scale installations to

429 remove H₂S from gas streams in which thiols and diorgano polysulfanes are present (Janssen
430 et al. 1998).

431

432

433 **Acknowledgements**

434 This work was performed within the cooperation framework of Wetsus, European
435 Centre of Excellence for Sustainable Water Technology (www.wetusus.nl). Wetusus is co-
436 funded by the Netherlands' Ministry of Economic Affairs and Ministry of Infrastructure and
437 the Environment, the European Union's Regional Development Fund, the Province of
438 Fryslân, and the Northern Netherlands Provinces. The authors thank the participants of the
439 research theme "Sulfur" and Paqell for fruitful discussions and financial support.

440 **References**

- 441 Anon, ALOGPS 2.1 software. Available at: <http://www.vcclab.org/lab/alogps> [Accessed
442 2015].
443
- 444 Van den Bosch, P.L.F., de Graaff, M., Fortuny-Picornell, M., van Leerdam, R.C., Janssen,
445 A.J.H., 2009. Inhibition of microbiological sulfide oxidation by methanethiol and dimethyl
446 polysulfides at natron-alkaline conditions. *Appl. Microbiol. Biotechnol.* 83 (3), 579–587.
447
- 448 Cline, C., Hoksberg, A., Abry, R., Janssen, A.J.H., 2003. Biological Process for H₂S
449 Removal from Gas Streams: The Shell-Paques/THIOPAQ™ Gas Desulfurization Process.
450 In *Proceedings of the Laurance Reid Gas Conditioning Conference*. p. 1–18.
451
- 452 Cronin, M.T., 2004. *Predicting chemical toxicity and fate*, CRC press.
453
- 454 Cui, H., Turn, S.Q., Reese, M.A., 2009. Removal of sulfur compounds from utility pipelined
455 synthetic natural gas using modified activated carbons. *Catal. Today* 139 (4), 274–279.
456
- 457 Graaff, C. de, 2012. *Biological treatment of sulfidic spent caustics under haloalkaline*
458 *conditions using soda lake bacteria*, Thesis Wageningen University.
459
- 460 Gregersen, L.H., Bryant, D.A., Frigaard, N.-U., 2011. Mechanisms and evolution of oxidative
461 sulfur metabolism in green sulfur bacteria. *Front. Microbiol.* 2.
462
- 463 Janssen, A.J.H., Lens, P.N.L., Stams, A.J.M., Plugge, C.M., Sorokin, D.Y., Muyzer, G.,
464 Dijkman, H., Van Zessen, E., Luimes, P., Buisman, C.J.N., 2009. Application of bacteria
465 involved in the biological sulfur cycle for paper mill effluent purification. *Sci. Total*
466 *Environ.* 407 (4), 1333–1343.
467
- 468 Janssen, A.J.H., Meijer, S., Bontsema, J., Lettinga, G., 1998. Application of the redox
469 potential for controlling a sulfide oxidizing bioreactor. *Biotechnol. Bioeng.* 60 (2), 147–155.
470
- 471 Keesman, K.J., 2011. *System identification: an Introduction*, Springer, Verlag, UK.
472
- 473 Kim, K.-H., Choi, Y., Jeon, E., Sunwoo, Y., 2005. Characterization of malodorous sulfur
474 compounds in landfill gas. *Atmos. Environ.* 39 (6), 1103–1112.
475
- 476 Kleinjan, W.E., Keizer, A. de, Janssen, A.J., 2005. Kinetics of the chemical oxidation of
477 polysulfide anions in aqueous solution. *Water Res.* 39 (17), 4093–4100.
478
- 479 Klok, J., de Graaff, M., van den Bosch, P.L.F., Boelee, N.C., Keesman, K.J., Janssen, A.J.H.,
480 2013. A physiologically based kinetic model for bacterial sulfide oxidation. *Water Res.*
481 47(2), 483–492.
482
- 483 Klok, J.B.M., van den Bosch, P.L.F., Buisman, C.J.N., Stams, A.J.M., Keesman, K.J.,
484 Janssen, A.J.H., 2012. Pathways of sulfide oxidation by haloalkaliphilic bacteria in limited-
485 oxygen gas lift bioreactors. *Environ. Sci. Technol.* 46 (14), 7581–7586.
486
- 487 Lee, S., Xu, Q., Booth, M., Townsend, T.G., Chadik, P., Bitton, G., 2006. Reduced sulfur
488 compounds in gas from construction and demolition debris landfills. *Waste Manage.* 26

489 (5), 526–533.
490
491 Van Leerdam, R.C., Bosch, P.L.F., Lens, P.N.L., Janssen, A.J.H., 2011. Reactions between
492 methanethiol and biologically produced sulfur. *Environ. Sci. Technol.* 45 (4), 1320–1326.
493
494 Marangoni, A.G., 2003. *Enzyme kinetics: a modern approach*, John Wiley & Sons.
495
496 Mora, M., López, L.R., Lafuente, J., Pérez, J., Kleerebezem, R., van Loosdrecht, M.C.,
497 Gamisans, X., Gabriel, D., 2016. Respirometric characterization of aerobic sulfide,
498 thiosulfate and elemental sulfur oxidation by S-oxidizing biomass. *Water Res.* 89, 282–
499 292.
500
501 Muyzer, G., Sorokin, D.Y., Mavromatis, K., Lapidus, A., Clum, A., Ivanova, N., Pati, A., d'
502 Haeseleer, P., Woyke, T., Kyrpides, N.C., 2011. Complete genome sequence of
503 “Thioalkalivibrio sulfidophilus” HL-EbGr7. *Stand. Genomic. Sci.* 4 (1), 23.
504
505 Pfennig, N., Lippert, K.D., 1966. Über das vitamin B₁₂-bedürfnis phototropher
506 Schwefelbakterien. *Arch. Microbiol.* 55 (3), 245–256.
507
508 Roman, P., Bijmans, M.F.M., Janssen, A.J.H., 2015a. Influence of methanethiol on biological
509 sulfide oxidation in gas treatment system. *Environ. Tech.* (just-accepted), 1–42.
510
511 Roman, P., Veltman, R., Bijmans, M.F.M., Keesman, K., Janssen, A.J.H., 2015b. Effect of
512 methanethiol concentration on sulfur production in biological desulfurization systems
513 under haloalkaline conditions. *Environ. Sci. Technol.* 49, 9212–9221.
514
515 Roosta, A., Jahanmiri, A., Mowla, D., Niazi, A., 2011. Mathematical modeling of biological
516 sulfide removal in a fed batch bioreactor. *Biochem. Eng. J.* 58, 50–56.
517
518 Schieder, D., Quicker, P., Schneider, R., Winter, H., Prechtel, S., Faulstich, M., 2003.
519 Microbiological removal of hydrogen sulfide from biogas by means of a separate biofilter
520 system: experience with technical operation. *Water Sci. Technol.* 48 (4), 209–212.
521
522 Segal, I., 1993. *Enzyme Kinetics: Behavior and Analysis of Rapid Equilibrium and Steady-*
523 *State Enzyme Systems*, Wiley, New York, USA.
524
525 Sorokin, D., van den Bosch, P.L.F., Abbas, B., Janssen, A.J.H., Muyzer, G., 2008.
526 Microbiological analysis of the population of extremely haloalkaliphilic sulfur-oxidizing
527 bacteria dominating in lab-scale sulfide-removing bioreactors. *Appl. Microbiol. Biotechnol.*
528 80 (6), 965–975.
529
530 Sorokin, D.Y., Banciu, H., Robertson, L.A., Kuenen, J.G., Muntyan, M.S., Muyzer, G., 2013.
531 Halophilic and haloalkaliphilic sulfur-oxidizing bacteria. In Rosenberg E. et al., ed. *The*
532 *Prokaryotes*. Springer-Verlag: Berlin-Heidelberg, p. 529–554.
533
534 Sorokin, D.Y., Banciu, H.L., Muyzer, G., 2015. Functional microbiology of soda lakes. *Curr.*
535 *Opin. Microbiol.* 25, 88–96.
536

- 537 Sorokin, D.Y., Kuenen, J.G., Muyzer, G., 2011. The microbial sulfur cycle at extremely
538 haloalkaline conditions of soda lakes. *Front. Microbiol.*, 2 (article 44), March 2011.
539
- 540 Sorokin, D.Y., Muntyan, M.S., Panteleeva, A.N., Muyzer, G., 2012. Thioalkalivibrio
541 sulfidophilus sp. nov., a haloalkaliphilic, sulfur-oxidizing gammaproteobacterium from
542 alkaline habitats. *Int. J. Syst. Evol. Microbiol.* 62 (Pt 8), 1884–1889.
543
- 544 Steudel, R., 2002. The chemistry of organic polysulfanes RS (n)-R (n> 2). *Chem. Rev.* 102
545 (11), 3905.
546
- 547 Tetko, I.V., Tanchuk, V.Y., 2002. Application of associative neural networks for prediction of
548 lipophilicity in ALOGPS 2.1 program. *J. Chem. Inf. Comp. Sci.* 42 (5), 1136–1145.
549
- 550 Wilms, J., Lub, J., Wever, R., 1980. Reactions of mercaptans with cytochrome c oxidase and
551 cytochrome c. *Biochim. Biophys. Acta, Bioenerg.* 589 (2), 324–335.
552
- 553 Yung-Chi, C., Prusoff, W.H., 1973. Relationship between the inhibition constant (K_i) and the
554 concentration of inhibitor which causes 50 per cent inhibition (I₅₀) of an enzymatic
555 reaction. *Biochem. Pharmacol.* 22 (23), 3099–3108.
556
- 557 Zannoni, D., others, 2004. *Respiration in archaea and bacteria*, Springer.
558
- 559 Zhang, S., Zhao, H., John, R., 2001. A theoretical model for immobilized enzyme inhibition
560 biosensors. *Electroanalysis* 13 (18), 1528–1534.
561
562

563 **TABLES**

564 **Table 1.** Chemicals used to prepare solutions in the current study. All chemicals were
565 purchased from Sigma-Aldrich, the Netherlands.

Compound name	CAS no.	Chemical formula	Solvent
Sodium sulfide hydrate	1313-84-4	$\text{Na}_2\text{S} \cdot 9 \text{H}_2\text{O}$	Water
Sodium thiomethoxide	5188-07-08	CH_3SNa	Water
Ethanethiol	75-08-1	$\text{C}_2\text{H}_5\text{SH}$	Methanol
1-Propanethiol	107-03-9	$\text{CH}_3\text{CH}_2\text{CH}_2\text{SH}$	Methanol
Dimethyl disulfide	624-92-0	$\text{CH}_3\text{S}_2\text{CH}_3$	Methanol
Diethyl disulfide	110-81-6	$(\text{C}_2\text{H}_5)_2\text{S}_2$	Methanol
Dipropyl disulfide	629-19-6	$(\text{CH}_3\text{CH}_2\text{CH}_2)_2\text{S}_2$	Methanol

566

567 **Table 2.** Concentration of inhibitors (C_i) and incubation time (T) used in sulfide-dependent
 568 respiration tests for assessing the oxygen consumption rates R1 and R2.

Inhibitor	R1		R2	
	C_i [mM]	T [min]	C_i [mM]	T [min]
Methanethiol	0.024	5	0.005	2
Ethanethiol	0.061	5	0.025	6
Propanethiol	0.080	15	0.017	15
Dimethyl disulfide	0.960	10	0.100	20
Diethyl disulfide	1.200	10	0.100	15
Dipropyl disulfide	0.850	25	0.420	10

569

570 **Table 3.** Estimated specific maximal reaction rate (r_{max}), Michaelis-Menten constant (K_M) and
571 inhibition constants (K_i and K_{ies}) with their corresponding standard deviation (σ) for the first
572 (R1) and second (R2) oxygen consumption rates.

Reaction rate	Inhibitor	Mode of inhibition	Parameter	Estimated value	σ	Unit
R1 ($\text{HS}^- \rightarrow \{\text{S}_x\}$)	Not inhibited reaction		r_{max}	600	30	$\mu\text{M O}_2 \text{ (mg N h)}^{-1}$
			K_M	79	9	μM
	MT	competitive	K_i	23	2	μM
	ET		K_i	46	5	μM
	PT		K_i	50	6	μM
	DMDS	uncompetitive	K_{ies}	1000	90	μM
	DEDS		K_{ies}	710	60	μM
	DPDS		K_{ies}	440	20	μM
R2 ($\{\text{S}_x\} \rightarrow \text{SO}_4^{2-}$)	Not inhibited reaction		r_{max}	103	4	$\mu\text{M O}_2 \text{ (mg N h)}^{-1}$
			K_M	1.9	0.4	μM
	MT	mixed	K_i	5	2	μM
			K_{ies}	14	3	μM
	ET		K_i	8.2	0.8	μM
			K_{ies}	40	3	μM
	PT		K_i	10	2	μM
			K_{ies}	70	10	μM
	DMDS	mixed	K_i	49	6	μM
			K_{ies}	260	20	μM
	DEDS		K_i	61	6	μM
			K_{ies}	230	20	μM
	DPDS		K_i	100	10	μM
			K_{ies}	220	10	μM

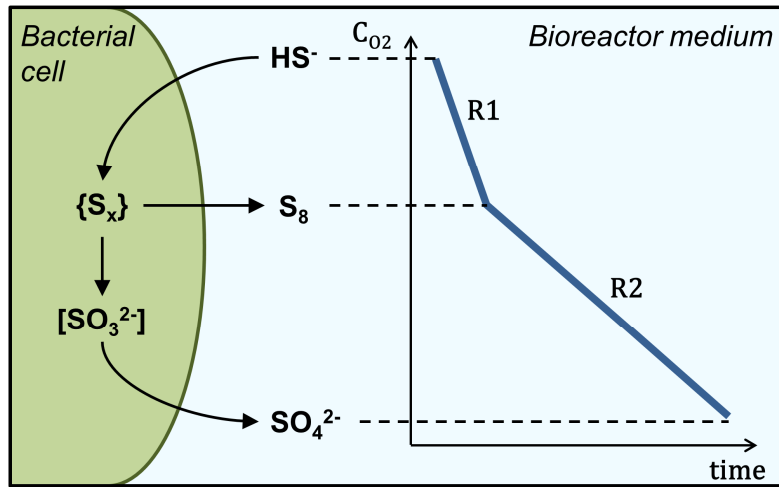
573

574 **Table. 4.** Calculated IC₅₀ values for methanethiol and dimethyl disulfide, and comparison
 575 with literature data at sulfide concentration of 0.2 mM.

IC ₅₀ [mM]		pH	[Na ⁺ + K ⁺]	Reference
Methanethiol	Dimethyl disulfide			
0.08 ± 0.01	1.4 ± 0.1	9	1	current study
0.05	1.5	9	2	(van den Bosch et al. 2009)
0.11 ± 0.02	N.A.	8.5	1.5	(Roman et al. 2015a)
0.2 ± 0.6	1.4 ± 0.2	9.5	0.8	(Graaff 2012)

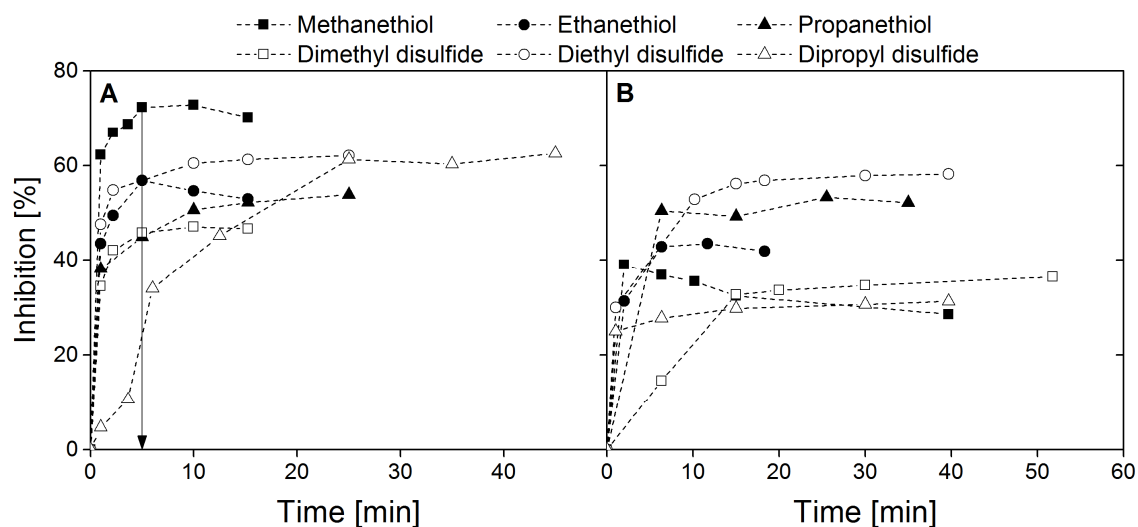
576 N.A. – not available

577 **FIGURES**



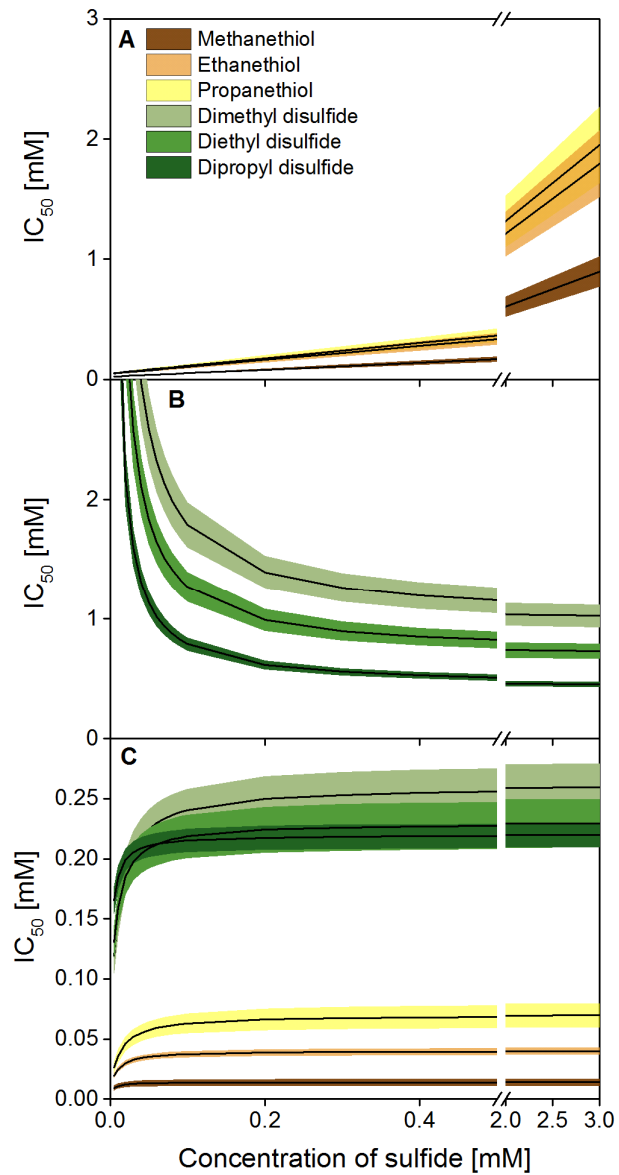
578

579 **Figure 1.** Schematic overview of the reaction that occurs in the bacterial cell related to sulfide
580 oxidation and the corresponding oxygen concentration profile from biological oxygen
581 measurements.



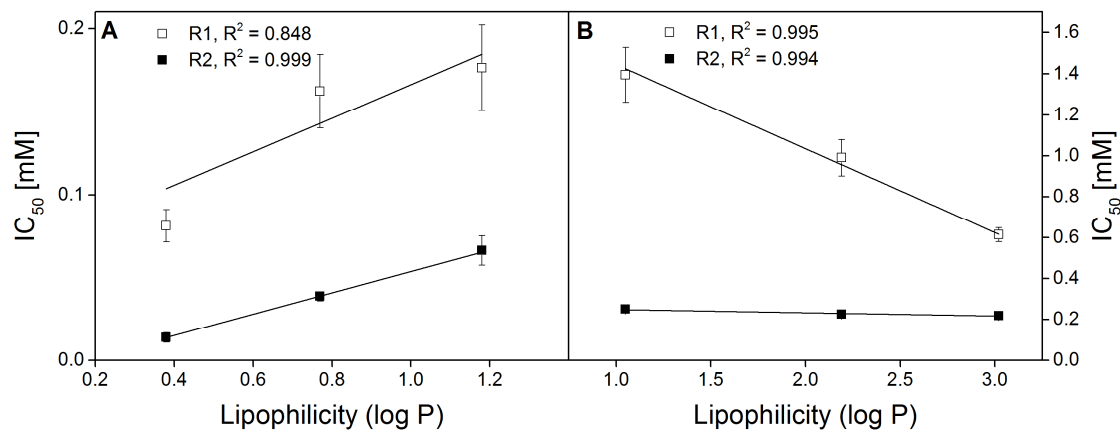
582

583 **Figure 2.** Incubation test performed to investigate time needed for complete saturation of
584 enzymes with inhibitor. **A.** Inhibition results for the first rate of the oxygen consumption rate.
585 Concentrations of methanethiol, ethanethiol, propanethiol, dimethyl disulfide, diethyl
586 disulfide, dipropyl disulfide were equal to 0.0243, 0.06, 0.08, 0.96, 1.2 and 2.5 mM
587 respectively. The arrow indicates the incubation time used in tests with methanethiol. **B.**
588 Inhibition results for the second rate of the oxygen consumption rate. Concentrations of
589 methanethiol, ethanethiol, propanethiol, dimethyl disulfide, diethyl disulfide, dipropyl
590 disulfide were equal to 0.04, 0.01, 0.04, 0.1, 0.1 and 0.42 mM respectively. In all experiments
591 the biomass concentration was 10 mgN L^{-1} , $[\text{Na}^+ + \text{K}^+] = 1 \text{ M}$, $\text{pH} = 9$ and $T = 35 \text{ }^\circ\text{C}$.



592

593 **Figure 3.** Calculated IC_{50} values with corresponding uncertainty bounds at increasing
 594 concentration of sulfide. **A.** Methanethiol, ethanethiol and propanethiol for the first oxygen
 595 consumption rate (R1). **B.** Dimethyl disulfide, diethyl disulfide and dipropyl disulfide (R1).
 596 **C.** All aforementioned inhibitors for the second oxygen consumption rate (R2).

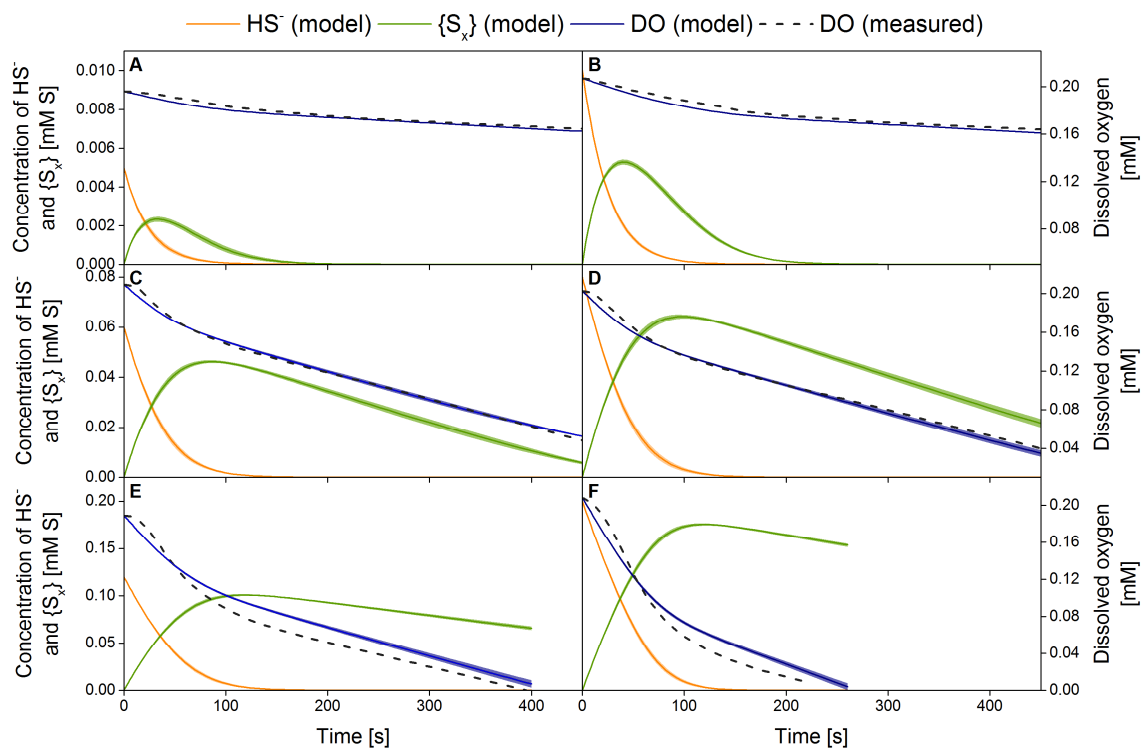


597

598 **Figure 4.** Relationship between lipophilicity and IC₅₀ values at sulfide concentration of 0.2

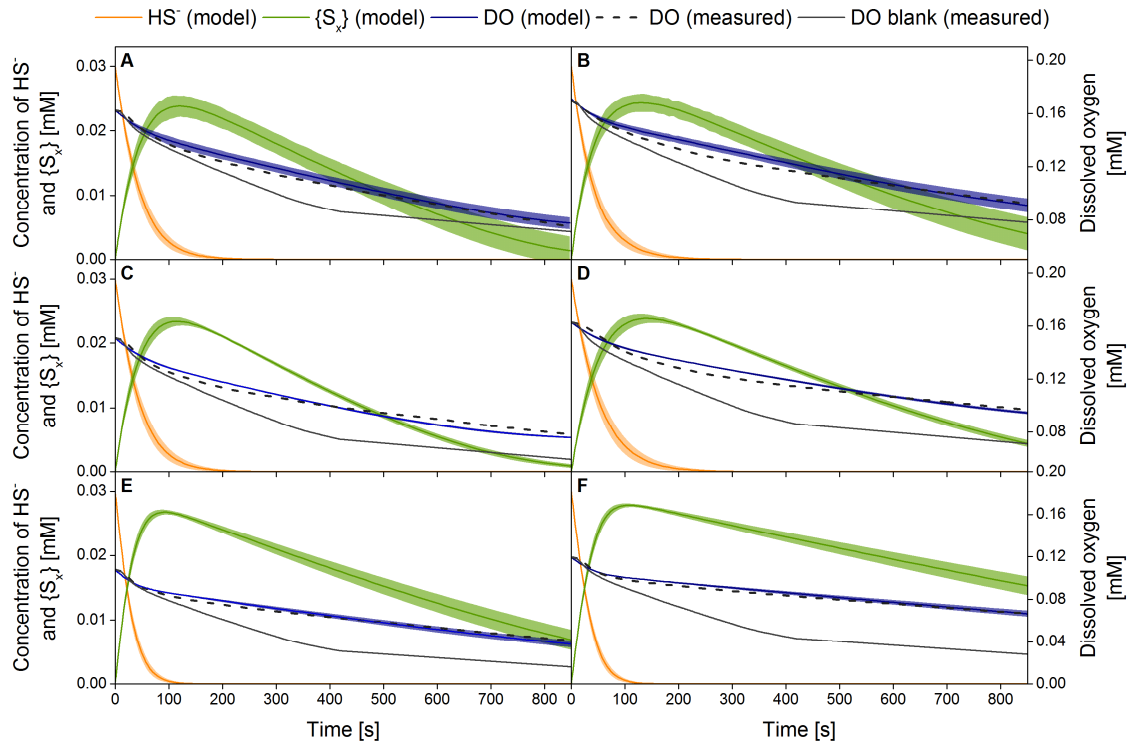
599 mM. **A.** Methanethiol, ethanethiol, propanethiol for the first (R1) and the second (R2) oxygen

600 consumption rate. **B.** Dimethyl disulfide, diethyl disulfide, dipropyl disulfide for R1 and R2.



601

602 **Figure 5.** Comparison between measured and predicted dissolved oxygen (DO) consumption
 603 rate and model predictions of sulfide (HS^-) and polysulfur compound $\{\text{S}_x\}$ concentrations, in
 604 absence of an inhibitor. Results of the simulation are based on estimates from Table 3. The
 605 sample interval is 1 s for both measured and predicted results. The initial sulfide
 606 concentration was 0.005, 0.01, 0.06, 0.08, 0.12, 0.2 mM in figures A-F, respectively. The
 607 biomass concentration was 10 mgN L^{-1} , $[\text{Na}^+ + \text{K}^+] = 1 \text{ M}$, $\text{pH} = 9$ and $T = 35 \text{ }^\circ\text{C}$.



608

609 **Figure 6.** Comparison between measured and predicted dissolved oxygen (DO) consumption
 610 rate and model predictions of sulfide (HS^-) and polysulfur compound $\{\text{S}_x\}$ concentration with
 611 corresponding model output uncertainties as a result of variations in estimated parameters.
 612 Results of the simulation are based on estimates from Table 3. The sample interval is 1 s for
 613 both measured and predicted results. Respiration test were performed at different
 614 concentration of various inhibitors: **A.** Methanethiol, 0.02 mM. **B.** Methanethiol, 0.04 mM. **C.**
 615 Ethanethiol, 0.04 mM. **D.** Ethanethiol, 0.08 mM. **E.** Dimethyl disulfide, 0.5 mM. **F.** Dimethyl
 616 disulfide, 1 mM. DO blank refers to an experiment performed without inhibitor. The biomass
 617 concentration was 10 mgN L^{-1} , $[\text{Na}^+ + \text{K}^+] = 1 \text{ M}$, $\text{pH} = 9$ and $T = 35 \text{ }^\circ\text{C}$.

Supplementary Information

S1. Figures:

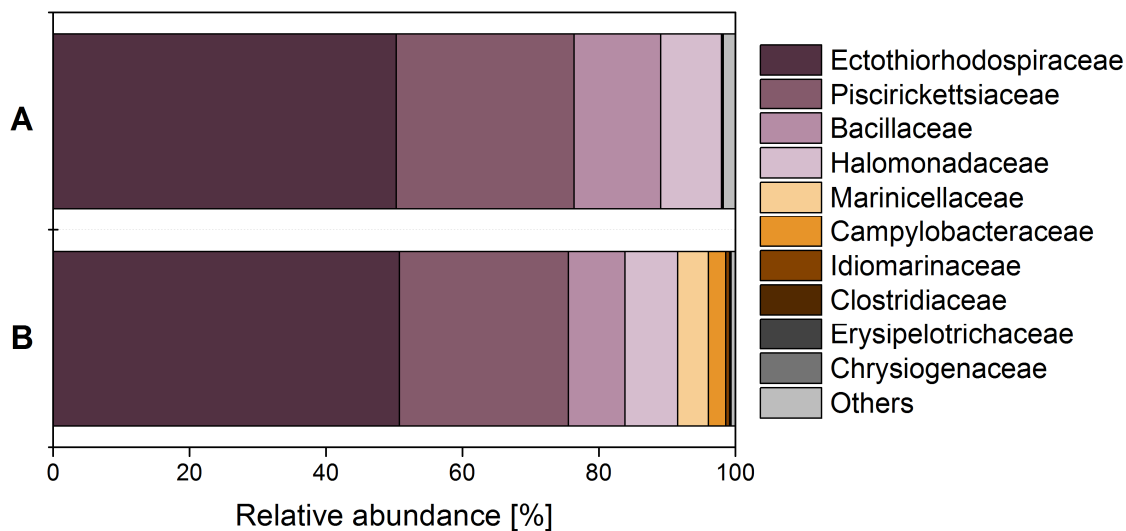


Figure S1. Relative abundance of the microbial composition based on the 16S rRNA gene for the biomass from a full-scale gas biodesulfurization installation (Janssen et al. 2009). Only bacteria with a relative abundance higher than 0.5% are listed (remaining bacteria are grouped into “Others”). A and B represents two replicates.

★ Uninhibited ■ Methanethiol ● Ethanethiol ▲ Propanethiol
 □ Dimethyl disulfide ○ Diethyl disulfide ☆ Uninhibited (for dipropyl disulfide) △ Dipropyl disulfide

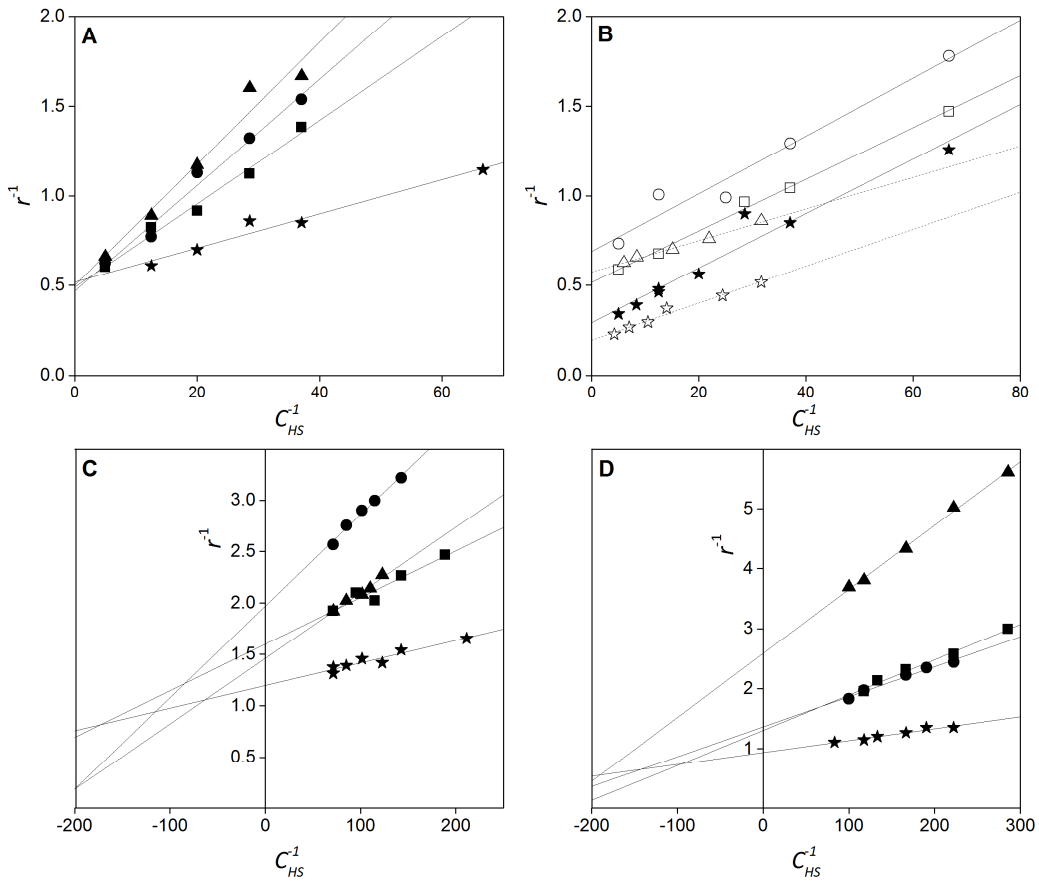
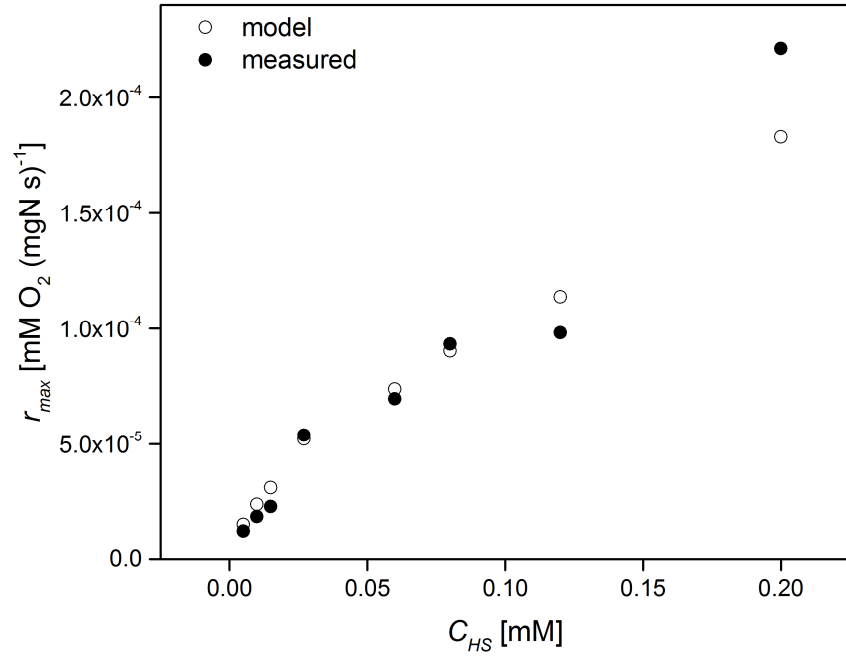


Figure S2. An example of results from sulfide-dependent respiration tests plotted on double-reciprocal plots for the first (A and B) and the second (C and D) oxygen consumption rate, where r is the reaction rate ($\text{mM O}_2 (\text{mg N h})^{-1}$) and C_{HS} is the sulfide concentration (mM). The inhibitors concentrations for each oxygen consumption rate are given in Table 2. The biomass concentration was 10 mg N L^{-1} , $\text{pH} = 9$ and $T = 35 \text{ }^\circ\text{C}$.



1

2 **Figure S3.** Comparison between measured and predicted reaction rate for the first rate of the
3 oxygen consumption rate at different initial sulfide concentrations.

4 **S2. Covariance and correlation matrix of the estimates**

5 The parameter estimates related to the first oxygen consumption rate (R1) are given by:

6
$$\hat{\theta}_{R1} = \begin{pmatrix} r_{max}^{R1} \\ K_m^{R1} \end{pmatrix} = \begin{pmatrix} 0.6 \\ 0.079 \end{pmatrix}$$

7 with corresponding covariance and correlation matrices:

8
$$COV_{\hat{\theta}_{R1}} = \begin{pmatrix} 0.0012 & 0.0003 \\ 0.0003 & 0.0001 \end{pmatrix}$$

9
$$R_{\hat{\theta}_{R1}} = \begin{pmatrix} 1 & 0.866 \\ 0.866 & 1 \end{pmatrix}$$

10 Similarly, parameters estimates related to the second oxygen consumption rate (R2) are

11 described by:

12
$$\hat{\theta}_{R2} = \begin{pmatrix} r_{max}^{R2} \\ K_m^{R2} \end{pmatrix} = \begin{pmatrix} 0.103 \\ 0.0019 \end{pmatrix}$$

13
$$COV_{\hat{\theta}_{R2}} = \begin{pmatrix} 0.0000148 & 0.0000019 \\ 0.0000019 & 0.0000003 \end{pmatrix}$$

14
$$R_{\hat{\theta}_{R2}} = \begin{pmatrix} 1 & 0.864 \\ 0.864 & 1 \end{pmatrix}$$

15